Evaluating Safety Envelope for Bus-VRU Interactions: Passenger and VRU Perceived Safety Implication

Downloaded from: https://research.chalmers.se, 2026-09-07 18:10 UTC

Citation for the original published paper (version of record):
Elawad, A., Murgovski, N., Kovaceva, J. (2026). Evaluating Safety Envelope for Bus-VRU Interactions: Passenger and VRU Perceived Safety
Implication. Transportation Research Procedia, 95: 41-48.
http://dx.doi.org/10.1016/j.trpro.2026.02.006

N.B. When citing this work, cite the original published paper.

research.chalmers.se offers the possibility of retrieving research publications produced at Chalmers University of Technology. It covers all kind of research output: articles, dissertations, conference papers, reports etc. since 2004. research.chalmers.se is administrated and maintained by Chalmers Library

(article starts on next page)

Available online at www.sciencedirect.com

ScienceDirect

Transportation Research Procedia 95 (2026) 41–48

Transportation Research Procedia

www.elsevier.com/locate/procedia

Euro Working Group on Transportation Annual Meeting 2025 - EWGT2025

Evaluating Safety Envelopes for Bus-VRU Interactions: Passenger and VRU Perceived Safety Implications

Amal Elawad[a,*], Nikolce Murgovski[a], Jordanka Kovaceva[b]

[a]*Mechatronic Research Group, Department of Electrical Engineering, Chalmers University of Technology, 412 96 Gothenburg, Sweden*
[b]*Division of Vehicle Safety, Department of Mechanics and Maritime Sciences, Chalmers University of Technology, 412 96 Gothenburg, Sweden*

Abstract

Buses are an essential means of urban transportation and are generally considered safe. However, accidents involving buses can cause severe injuries and fatalities to a Vulnerable Road User (VRU). This study introduces a novel method to compute safety envelopes, which are sets characterized by the closest longitudinal distance to a VRU, where an intervention can still be initiated to avoid a bus-to-VRU collision — also known as the Minimum Safety Distance (MSD). Those envelopes are computed using reachability analysis and set volume optimization for automated bus collision avoidance systems. This research also shows how several factors — including the velocity of the vehicle upon VRU detection, simultaneous steering and braking maneuvers, and the perceived risks by both standing bus passengers and VRUs — influence the size of the safety envelopes. It also evaluates the MSD computed by our algorithm by comparing it to the unsafe distances observed in real-world bus-to-VRU crash data. Our key findings show the impact of the VRU-Perceived Safety Risk (VRU-PSR) on the critical set, which refers to the set outside the safety envelope. For an initial speed of 60 km/h, the MSD was found to decrease by 3.7 m when the VRU-PSR increased from dangerous risk to the highest risk. Additionally, the Passenger-Perceived Safety Risk (P-PSR) was found to significantly affect the critical set, as it allows for more aggressive maneuvers. For instance, for a fixed lateral offset and VRU-PSR, when the permitted P-PSR is increased from 75% to 100%, the MSD decreased by 5 m and 1.4 m, for initial velocities of 20 km/h and 50 km/h, respectively. Furthermore, the evaluation of our computed MSD against crash data revealed that the braking distances recorded for crashes, with one exception, fell within our critical set. This demonstrates that operating within the computed critical sets does correspond to crashes, as compared to the performance of professional drivers.

© 2026 The Authors. Published by ELSEVIER B.V.
This is an open access article under the CC BY-NC-ND license (https://creativecommons.org/licenses/by-nc-nd/4.0)
Peer-review under responsibility of the scientific committee of the Euro Working Group on Transportation Annual Meeting 2025 - EWGT2025.

Keywords: Set volume optimization; reachability analysis; safety envelope; critical set; bus; VRU comfort; passenger comfort; minimum safe distance; collision avoidance

* Corresponding author.
E-mail address: amal.a.elawad@gmail.com

2352-1465 © 2026 The Authors. Published by ELSEVIER B.V.
This is an open access article under the CC BY-NC-ND license (https://creativecommons.org/licenses/by-nc-nd/4.0)
Peer-review under responsibility of the scientific committee of the Euro Working Group on Transportation Annual Meeting 2025 - EWGT2025.
10.1016/j.trpro.2026.02.006

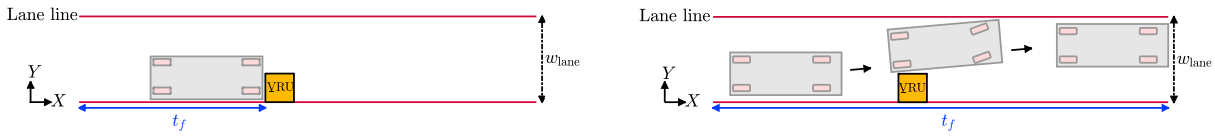

(a) Stopping before the VRU (SB)

(b) Stopping after the VRU (SA)

Fig. 1: The bus brakes and steers to avoid collision with the VRU either by (a) stopping before, or (b) stopping after the VRU. The road is assumed to have multiple lanes, the width of the lane is given by w_{lane}, and the origin of the inertial coordinates (X_0, Y_0) is given by the intersection of the bottom left edge of the VRU with the right edge of the road. The bus vs. lane width is scaled for illustration.

1. Introduction

Buses are widely regarded as a safe and essential mode of urban transportation (Kendall et al., 1994). However, accidents involving buses, especially in densely populated areas, remain a significant issue and often result in severe injuries and fatalities among Vulnerable Road Users (VRUs) (Schindler and Jeppsson, 2024). To reduce the number of crashes and injuries for both bus passengers and VRUs, systems such as the Advanced Driver Assistance System (ADAS) and automated driving functions are developed. As in Dahl et al. (2018), ADAS functionalities include sensing and estimation, threat assessment/decision-making, and actuation to perform the maneuver. The scope of this paper concerns methods for the latter two. One method for threat assessment is to determine the last point in time after which no evasive maneuver is feasible. This is commonly computed using set-based approaches combined with single-behavior threat metrics — such as Time to Collision (TTC) or Minimum Safe Distance (MSD). This combination is often referred to as a distance-based safety boundary or safety envelope of vehicle-VRU collision avoidance, as given in Dahl et al. (2018) and Erlien et al. (2015), where computations of the safety envelope have been studied. For actuation, autonomous braking and steering systems that try to avoid or mitigate collisions with VRUs can be implemented. In the previous studies, the influence of the perceived safety risk of the passengers and VRUs on the computation of the safety envelope has not been investigated. Moreover, maneuvers involving simultaneous steering and braking for collision avoidance in buses were not previously studied.

The contribution of this study is to: 1) develop a novel method to compute the safety envelope effectively through reachability analysis and set volume optimization; 2) investigate how the size of the safety envelope is impacted by simultaneous steering and braking maneuvers subject to constraints on the perceived risk by standing bus passengers and VRUs; and 3) investigate how the proposed MSD relates to unsafe distances recorded for bus-to-VRU collisions in real-world crash data.

2. Modeling and Problem Formulation

Computation of safety envelopes is a complex task, as it involves various factors like the vehicle model, perceived safety of passengers and VRUs, road constraints, and collision constraints with other road users. Moreover, the safety envelope may also be an open set, which is challenging to compute. Thus, we propose computing a critical set, which is a closed and bounded set, defined as the set difference between the vehicle set space and the safety envelope. It is also the volume of initial vehicle states from which a collision cannot be avoided, given the boundaries of the perceived safety of passengers and VRUs. The method of critical set computation can be described by the following scenario: an autonomous bus starting at some initial state x_0 is approaching a bus stop as a VRU is detected in its driving path. Here, it is assumed, without loss of generality, that the closest point of the VRU is at position zero. To avoid collisions with the VRU, an action needs to be made by emergency braking combined with evasive steering, and without: 1) exiting the driving lane – risking collisions with another vehicle; 2) exiting the road; and 3) exceeding the perceived risk of standing passengers or the VRU – risking passenger or VRU injury. A simultaneous braking and steering action can be performed either by stopping before the VRU (SB), see Fig. 1a, or by steering away and stopping after the VRU (SA), Fig. 1b.

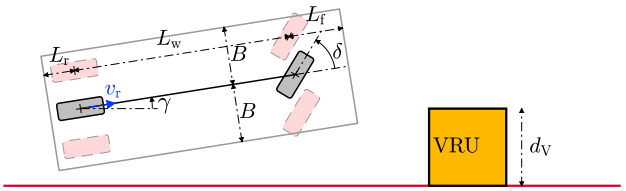

Fig. 2: The bus is modeled as a kinematic bicycle (bicycle wheels shown in solid lines), while the VRU is modeled as a rectangle with dimensions $d_v \times d_v$. The position of the bus on the road is determined by the distance of the mid-rear-axle point (x_r, y_r), longitudinally from the VRU and laterally from the right side of the road. The lengths L_f and L_r represent the front and rear overhang, respectively, L_w is the wheelbase, and B is half of the vehicle width.

2.1. The vehicle, passenger, and VRU models

In this study, the bus is modeled as a kinematic bicycle with 7 states and 2 control inputs, given by

$$\mathbf{x}(t) = \left[x_r(t)\ y_r(t)\ v_{xr}(t)\ a_{xr}(t)\ \gamma(t)\ \delta(t)\ \dot{\delta}(t)\right]^\top, \quad \mathbf{u}(t) = \left[j_{xr}(t)\ \ddot{\delta}(t)\right]^\top \tag{1}$$

where x_r and y_r represent the longitudinal and lateral components of bus position, respectively, v_{xr} is the longitudinal velocity, a_{xr} is the longitudinal acceleration, and γ is the heading angle; all measured at the mid-rear axle point. The steering angle and steering rate of the front bicycle wheel are given by δ and $\dot{\delta}$, respectively. The inputs are given by the longitudinal jerk, j_{xr}, and the steering acceleration, $\ddot{\delta}$. The subscripts $(\cdot)_r$ and $(\cdot)_x$ refer to the quantity being evaluated at the mid-rear axle point, and to a longitudinal quantity, respectively. The system dynamics are given by

$$\dot{\mathbf{x}}(t) = f(\mathbf{x}(t), \mathbf{u}(t)) = \left[v_{xr}(t)\cos(\gamma(t)) \quad v_{xr}(t)\sin(\gamma(t)) \quad a_{xr}(t) \quad j_{xr}(t) \quad v_{xr}(t)\tan(\delta(t))/L_w \quad \dot{\delta}(t) \quad \ddot{\delta}(t)\right]^\top \tag{2}$$

where L_w is the wheelbase. A rectangular shape models the VRU, and its position is assumed to be known within given margins, as the detection of the VRU position is beyond the scope of this study. The vehicle and VRU models are illustrated in Fig. 2.

For the risk perceived by the bus passengers, the analytical model from our previous work in Elawad et al. (2024) is utilized, which represents the percentage of standing passengers who perceive the ride as uncomfortable. The model is given by

$$f_{dis}(\mathbf{q}, a_i, j_i) = \frac{1 - e^{q_1|a_i| + q_2|j_i|}}{1 + e^{q_0 + q_1|a_i| + q_2|j_i|}}, \tag{3}$$

where a_i and j_i are the resultants of acceleration and jerk, respectively, the subscript $(\cdot)_i$ denotes the location along the bus where the quantity is evaluated (e.g., front, rear, and middle of the bus), and the parameter vector is given by $\mathbf{q} = \left[7.85\ -3.88\ -0.91\right]$. In this study, we are focusing on very high levels of discomfort (75% and above), which is hereafter referred to as the Passenger-Perceived Safety Risk (P-PSR).

The VRU-Perceived Safety Risk, denoted as VRU-PSR, is modeled using the Bayesian-Ordered Logistic Regression model developed previously by Rasch et al. (2022), given by

$$d(\mathbf{n}, p, v_{xr}) = \begin{cases} (-\log\frac{p}{1-p} + n_1 - n_3 v_{xr})\frac{1}{n_2}, & \text{dangerous risk} \\ 0, & \text{highest VRU risk} \end{cases} \tag{4}$$

where d is the distance to the vehicle, p is the threshold for the perceived dangerous risk, and the parameter vector is given by $\mathbf{n}=\begin{bmatrix}1.24 & -4 & 0.23\end{bmatrix}$. Using p=80% and the ego vehicle's speed, one can determine the distance to the VRU at which a maneuver would be perceived as posing a dangerous risk. For instance, an automated bus approaching a VRU would keep a lower speed when a larger distance cannot be achieved, ensuring the maneuver is perceived by the VRU as safe and of low risk. The analytical model developed by Rasch et al. (2022) is, to our knowledge, one of the few frameworks that assess perceived risk of VRUs in interactions with vehicles, integrating both VRU perceived risk and kinematic vehicle measures. Although this model was originally developed using data from car-to-cyclist overtaking scenarios, it is applied here due to the absence of a similar model for bus-to-VRU interactions.

2.2. Problem formulation

The main objective of this paper is to maximize the volume of a safety envelope, which is an initial safe set defined by $\mathcal{X}_{\text{safe}}\subset\mathbb{X}_0$, where $\mathbb{X}_0$ is the set of all initial states. As long as the operation conditions are confined within this set, collisions with VRUs can still be avoided without violating the imposed constraints. The safe set $\mathcal{X}_{\text{safe}}$, may also be defined as the set of safe initial states, $\mathbb{X}_0$, for which there exists a control input that can lead the bus to the desired target set $\mathbb{X}_{\text{f}}$. The target set is defined as the final longitudinal velocity and acceleration equal to zero, which is a reasonable assumption given that, in critical scenarios, it can be expected that the vehicle will eventually be driven to a standstill. This choice also ensures persistent feasibility, since once the vehicle reaches the target set, it can safely remain in it. The problem is formulated as an Optimal Control Problem (OCP), which can be expressed as

$$\max_{\mathbf{u},t_{\text{f}}} \text{Vol}(\mathcal{X}_{\text{safe}}) \tag{5a}$$

$$\text{s.t. } \dot{\mathbf{x}}(t) = f(\mathbf{x}(t),\mathbf{u}(t)), \qquad \forall t\in[0,t_{\text{f}}] \tag{5b}$$

$$g(\mathbf{x}(t),\mathbf{u}(t),\text{P}-\text{PSR},\text{VRU}-\text{PSR})\le 0, \qquad \forall t\in[0,t_{\text{f}}] \tag{5c}$$

$$\mathbf{x}_{\min}(t)\le\mathbf{x}(t)\le\mathbf{x}_{\max}(t), \qquad \forall t\in[0,t_{\text{f}}] \tag{5d}$$

$$\mathbf{u}_{\min}(t)\le\mathbf{u}(t)\le\mathbf{u}_{\max}(t), \qquad \forall t\in[0,t_{\text{f}}] \tag{5e}$$

$$\mathbf{x}(0)=\mathbf{x}_0\in\mathcal{X}_{\text{safe}}\subset\mathbb{X}_0 \tag{5f}$$

$$\mathbf{x}(t_{\text{f}})=\mathbf{x}_{\text{f}}\in\mathbb{X}_{\text{f}} \tag{5g}$$

$$t_{\text{f}}\in\mathbb{T}=[0,T_{\max}] \tag{5h}$$

with the final time given by t_{f}, the initial states by $\mathbf{x}_0$, the final states by $\mathbf{x}_{\text{f}}$, and the target set defined as $\mathbb{X}_{\text{f}}=\{\mathbf{x}_{\text{f}}\mid v_{\text{xr}}(t_{\text{f}})=0, a_{\text{xr}}(t_{\text{f}})=0\}$. Notice that t_{f} in the problem is not fixed, but rather stated as a decision variable to be computed. The reason is that the vehicle may choose different ways to avoid collisions, e.g., SB or SA. In the latter scenario, we let the final time span up to a maximum value $T_{\max}$ within a set of travel time $\mathbb{T}$, which is chosen large enough to not significantly affect the safe set, while eventually bringing the vehicle to a standstill. The optimization is subject to multiple constraints, namely the box constraints in (5d) and (5e), for states and inputs, respectively, and the general constraints in (5c). The latter includes the geometric constraints, for collision avoidance, and the passenger and VRU comfort constraints. The comfort constraints are given by

$$\begin{bmatrix}0\\0\end{bmatrix}\le\begin{bmatrix}f_{\text{dis}}(\mathbf{q},a_i,j_i)\\ d(\mathbf{n},p,v_{\text{xr}})\end{bmatrix}\le\begin{bmatrix}\text{P}-\text{PSR}\\ \text{VRU}-\text{PSR}\end{bmatrix}. \tag{6}$$

To the left, the vehicle is geometrically constrained by the lane line, preventing crossings to the adjacent lane (see Fig. 1). To the right, and when passing by the VRU, the vehicle is constrained by the VRU rectangle. The geometric constraints are imposed using the Hyperplane method given in our previous work Fan et al. (2024). This gives box constraints and general inequality constraints, which together with (6) are expressed as (5c)-(5e).

The constraints on states and input are given by the vehicle's physical limits. For system dynamics, those are $a_{xr}= \pm 9\,\mathrm{m/s^2}$ and $j_{xr}= \pm 20\,\mathrm{m/s^3}$ (Knight et al., 2019). For passenger vehicles, the limits of the steering angle δ are around $\pm 45\,^\circ$. The steering rate is around $\pm 10\,^\circ/\mathrm{s}$, for an automated steering function. The limits for steering acceleration depend on the driving situation and the type of vehicle. Assuming a net moment of 100 Nm and inertia of $0.1\,\mathrm{kgm^2}$, one would get $\ddot{\delta}=50\,^\circ/\mathrm{s^2}$ — given that the steering ratio is around 20 for a single-story bus. It must be noted that those maximum limits still guarantee safe vehicle operation, although possibly highly uncomfortable. Thus, reaching those limits is confined by the comfort models of the passengers and the VRU.

The volume function in the objective is stated here only as a construct that provides a scalar measure of the set. In the following section, the implementation of this function can actually be circumvented. In addition, problem (5) is difficult to solve exactly, as it is nonlinear, non-convex, infinitely dimensional, and with free initial and final positions and final time. A common way of approaching such OCPs entails approximating the problem by transcribing it to a discrete space, among other measures, which is discussed further in the following section.

3. Computation of critical sets

The safety envelope can, in principle, be identified using backward reachability, propagating backward from the target set $\mathbb{X}_\mathrm{f}$, depending on the position of the vehicle on the road, the perceived safety risks, and the velocity upon VRU detection. The backward iteration is terminated when the states finally reach $\mathcal{X}_\mathrm{safe}$, where interventions to avoid collisions are still feasible.

A numerical solution is sought by discretizing the continuous time variables, conventionally with respect to time. However, for the problem at hand, t_f is bounded but unknown. Another approach in Elawad et al. (2021) is discretizing with respect to the traveled distance. However, $x_\mathrm{r}(0)$ is also unknown a priori. Therefore, a new independent variable needs to be identified, namely, normalized time $\tau \in [0, 1]$. This variable is connected to the physical time by $t=\tau \cdot t_\mathrm{f}$, and allows redefining the system dynamics as functions of the normalized time τ,

$$\mathbf{x}'(\tau) = \frac{\mathrm{d}\mathbf{x}(\tau)}{\mathrm{d}\tau} = \frac{\mathrm{d}\mathbf{x}(t)}{\mathrm{d}t} \cdot \frac{\mathrm{d}t}{\mathrm{d}\tau} = \dot{\mathbf{x}}(t) \cdot t_\mathrm{f} = t_\mathrm{f} \cdot f(\mathbf{x}(\tau), \mathbf{u}(\tau)). \tag{7}$$

Note that an identical solution to the problem (5) can be obtained by minimizing the volume of unsafe initial states. Let this set be denoted as the critical set, given by the set difference

$$\mathcal{X}_\mathrm{c} = \mathbb{X}_0 \backslash \mathcal{X}_\mathrm{safe}. \tag{8}$$

The critical set is a nine-dimensional object, including all the states and inputs, see Eq. (1), and the additional two dimensions for the perceived risks. The volume of the critical sets is impacted the most by the perceived risks, the longitudinal and lateral positions, and the longitudinal speed. Therefore, the optimization is focused on variational analyses of these quantities. The volume of the critical set is smaller than that of the safe set. Hence, variational analyses of quantities minimizing the critical set reduce the computational load. The computation can be further improved by effectively reducing one dimension, by letting the optimal control and trajectory planning algorithm decide on the control actions and maneuvering time to minimize the longitudinal distance to the VRU, from which a collision is still avoidable. The MSD between the vehicle and VRU is computed, which can be written as $\min_\mathbf{u} -x_\mathrm{r}(0)$, with $x_\mathrm{r}(0) \leq 0$, over a grid of values for initial vehicle lateral position and longitudinal speed, and risk levels for riders and VRUs.

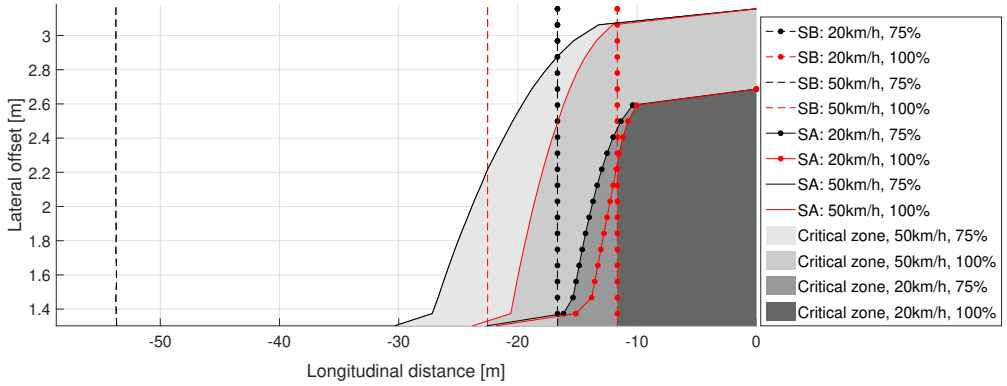

Fig. 3: Critical sets for SB and SA maneuver, with VRU-PSR dangerous, and P-PSR of 75% and 100%. The negative sign in the x-axis indicates the longitudinal distance before reaching the VRU, which is located at the origin.

4. Results and Discussions

4.1. Minimum volume of critical sets

For simulations, MATLAB R2023a was utilized, paired with the nonlinear optimization solver Interior Point Optimizer, *ipopt*, and CasADi, which is a numerical optimization framework developed by Andersson et al. (2019). Here, the results are provided for the critical set computed with initial bus speed range $v_0{=}v_{\mathrm{xr}}(0){\in}\{20, 50\}$ km/h, and lateral offset ranging from 1.28−4 m with step size of 0.09 m, while keeping all other vehicle states initialized to zero. The analysis of the size of the critical set was conducted for two levels of P-PSR, 75% and 100%, and with p=80% for the VRU-PSR. The analysis focused solely on complete collision avoidance, excluding crash severity mitigation.

Figure 3 shows the effect of the initial speed, passenger comfort, lateral distance to the VRU, and type of maneuver on the MSD and the size of the critical set. For instance, at an initial speed of v_0=50 km/h, P-PSR of 75%, and lateral offset of 2.3 m, the SA maneuver requires MSD of 21.9 m to avoid a collision with a VRU, in comparison to 53.7 m for the SB maneuver. In addition, allowing higher passenger discomfort significantly reduces the MSD for intervention in both maneuvers, since it allows for more aggressive maneuvers. This is observed in the red vs. black boundaries, representing P-PSR of 75% and 100%, respectively. To illustrate, it can be observed that for P-PSR of 100%, the MSD decreases to 17.5 m in comparison to the 21.9 m for 75%.

The size of the critical set is reduced with an increasing level of P-PSR. For instance, for v_0=50 km/h and P-PSR of 75% and 100%, the reduction of the required MSD ranges from 1.15 m to 6.7 m, depending on the lateral offset. This is shown by the lightest gray section in Fig 3. For those same conditions but at lower speeds, the difference in set volume is much smaller. For v_0=20 km/h, this ranges between 33 cm and 5 m. Moreover, it can be seen that in some cases, SA can be initiated later than SB while still avoiding a collision. For instance, at v_0=50 km/h, SA maneuver with P-PSR of 75% is avoiding the crash, even when SB with P-PSR of 100% is failing to prevent the crash, for lateral offset below 2.2 m. This can be seen in the black solid line for SA vs. the red dashed line for SB in Fig. 3.

4.2. Case study with accident data

To illustrate how the MSD relates to the unsafe distance observed in bus-to-VRU collisions, we conducted a case study using real-world crash data from the Initiative for the Global Harmonization of Accident Data (IGLAD) (Bakker et al., 2017). To focus on bus-to-pedestrian scenarios, the crash data was filtered to include crashes involving a single bus and a single pedestrian, in which the pedestrian is crossing the road — known as *crossing-type accidents* — with records of the initial speed of the bus and deceleration distance to the VRU. The dataset comprised 43 crashes, with 80% of these involving initial bus speeds below 50 km/h. We applied our method to compute the critical sets by using the actual initial bus speeds, v_0, recorded in the original crash. The lateral offset was set at 1.35 m, aligning the bus parallel to the road, with all other vehicle states initialized to zero. Then, the computed MSD was compared to the longitudinal distance recorded in the crashes. This is illustrated in Fig. 4, which shows the critical set with a P-PSR

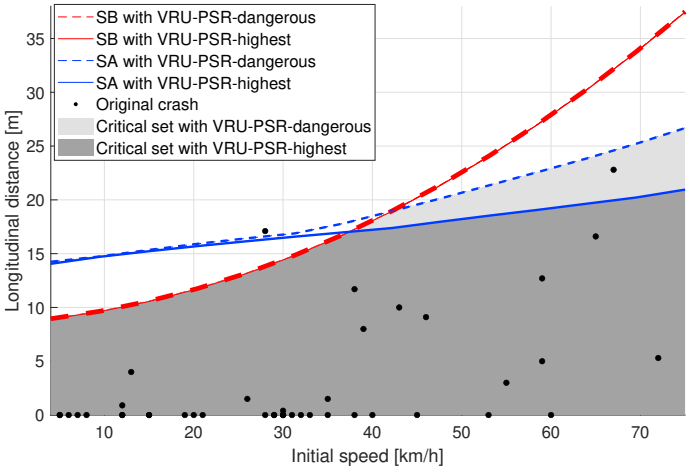

Fig. 4: Critical sets for lateral offset of 1.35 m and 100% P-PSR, for VRU-PSR-dangerous and VRU-PSR-highest. The dot markers indicate recorded accident data, represented by the initial speed and distance when deceleration started. The solid and dashed red lines overlap with a difference of 4.5 cm. The dark gray shaded area shows the critical-set-highest — a true subset of the critical-set-dangerous. Notice that for speed ranges above 40 km/h, SA maneuvers require shorter MSD for collision avoidance, in comparison to SB maneuvers.

of 100% and VRU-PSR at the dangerous and highest levels. The dark gray shaded area shows the critical set where the collision cannot be avoided, which is a true subset of the critical set-dangerous. The set difference between the critical-set-dangerous and critical-set-highest, which is the visible lighter gray area, shows the window where a system would need to engage to avoid the collision.

As recorded in the crash data, all maneuvers required longer MSD than the actual distance when the bus drivers began decelerating. All deceleration distances, except for one, fell within the critical set. This outlier is shown in Fig. 4 at the initial speed of 28 km/h, where the deceleration distance of 17.1 m would have been just enough to avoid the VRU with SA maneuver, which requires MSD of 16.3 m. In this crash case, the driver applied a deceleration of 3.5 m/s^2, which was insufficient to avoid the collision. It would also have been possible to avoid the collision with the SB maneuver, which requires 13.8 m, if the driver had applied greater braking force or an automated system had engaged. Another point at an initial speed of 67 km/h and a distance of 22.8 m is above the boundary of critical-set-highest, which could have been possible to avoid with an SA maneuver with MSD of 20 m. However, in this crash, the driver applied only 6.5 m/s^2 of deceleration, which was insufficient to avoid a collision with the pedestrian. In addition, there were 27 crashes with zero recorded deceleration distances, indicating that the driver made no attempt to decelerate to avoid the VRU. In these cases, an automated system could potentially have avoided the collision or at least mitigated the severity of the impact.

The maneuvers where the VRU-PSR-dangerous model is implemented require a longer MSD to avoid collisions with the VRU, as opposed to those with the VRU-PSR-highest model. For the SB maneuver, the MSD increased by a maximum of 4.5 cm with the VRU-PSR-dangerous compared to VRU-PSR-highest. For the SA maneuver, the MSD increased by up to 5.7 m. Also, for speed ranges above 40 km/h, SA maneuvers require shorter MSD for collision avoidance, in comparison to SB maneuvers.

5. Conclusion and Future Work

In this paper, we provided a method to compute the size of the critical set, by simultaneous steering and braking maneuvers, subject to constraints on the perceived risk by VRUs and standing bus passengers. Consistent with expectations, the inclusion of the P-PSR and VRU-PSR required longer MSD to initiate steering and braking maneuvers, compared to cases without these models. Allowing higher P-PSR reduced the volume of the critical set. Depending on the lateral offset to the VRU and the initial speed, increasing P-PSR from 75% to 100% decreased the MSD by the range of 1.15-6.7 m for initial speed of 50 km/h, and 33 cm-5 m for initial speed of 20 km/h. Increasing the VRU-PSR from dangerous to highest risk reduced the size of the critical set, which is reflected by the decrease in the MSD. For

SB vs. SA maneuvers, the MSD decreased by 3.4 cm-4.5 cm vs. 3.4 cm-5.7 m, respectively — depending on the initial speed.

The comparison of the MSD to the crash data shows that, for a given initial speed, the braking distances recorded for the crashes, all except one, are within the critical set. This verifies that the computed critical sets coincide with the MSD of professional drivers in extreme evasive conditions, since even an automated system would not be able to avoid most of the crashes if initialized equivalently. However, the recorded data did not include information on detection delays of the VRU or reaction times of the drivers. If an automated system were capable of reacting earlier and executing a maneuver that would not only stop before the VRU but also perform an evasive steer-away maneuver, collisions might have been avoided, or the impact severity could have been mitigated. Given the levels for dangerous VRUs' and passengers' risks, the proposed method provides the interval when such systems should engage.

Acknowledgements

This research was supported by the Chalmers Transport Area of Advance project EFFECT.

References

Andersson, J.A., Gillis, J., Horn, G., Rawlings, J.B., Diehl, M., 2019. CasADi: A software framework for nonlinear optimization and optimal control. Mathematical Programming Computation 11, 1–36.

Bakker, J., Jeppsson, H., Hannawald, L., Spitzhüttl, F., Longton, A., Tomasch, E., 2017. IGLAD-international harmonized in-depth accident data, in: in Proceedings of the 25th International Conference on Enhanced Safety of Vehicles (ESV), Detroit, MI, pp. 1–12.

Dahl, J., de Campos, G.R., Olsson, C., Fredriksson, J., 2018. Collision avoidance: A literature review on threat-assessment techniques. IEEE Transactions on Intelligent Vehicles 4, 101–113.

Elawad, A., Murgovski, N., Jonasson, M., Sjöberg, J., 2021. Road boundary modeling for autonomous bus docking subject to rectangular geometry constraints, in: 2021 European Control Conference (ECC), IEEE. pp. 1745–1750.

Elawad, A., Murgovski, N., Jonasson, M., Sjöberg, J., 2024. Autonomous bus docking for optimal ride comfort of standing passengers. IEEE Transactions on Intelligent Transportation Systems .

Erlien, S.M., Fujita, S., Gerdes, J.C., 2015. Shared steering control using safe envelopes for obstacle avoidance and vehicle stability. IEEE Transactions on Intelligent Transportation Systems 17, 441–451.

Fan, J., Murgovski, N., Liang, J., 2024. Efficient optimization-based trajectory planning for unmanned systems in confined environments. IEEE Transactions on Intelligent Transportation Systems .

Kendall, I., Hassan, T., Bodiwala, G., 1994. A review of injuries sustained by bus passengers. Journal of Accident & Emergency Medicine 11, 57.

Knight, I., Dodd, M., Edwards, A., Edwards, M., Martin, P., McCarthy, M., 2019. The Transport for London Bus Safety Standard: Advanced Emergency Braking (AEB)-Evaluation of Safety Measure, TRL.

Rasch, A., Moll, S., López, G., Garcia, A., Dozza, M., 2022. Drivers' and cyclists' safety perceptions in overtaking maneuvers. Transportation Research Part F: Traffic Psychology and Behaviour 84, 165–176.

Schindler, R., Jeppsson, H., 2024. In-depth analysis of scenarios and injuries in crashes between cyclists and commercial vehicles in Germany. Traffic Safety Research 7, 1–13.